

# Acoustic Doppler Velocity Profiler for velocity and turbulence measurements in a large amplitude meandering flume

Donatella Termini<sup>1</sup> and Mafalda Piraino<sup>1\*</sup>

<sup>1</sup>Dipartimento di Ingegneria Idraulica ed Applicazioni Ambientali, University of Palermo, Viale delle Scienze, 90128 Palermo, Italy (\*Corresponding author, e-mail: [piraino@idra.unipa.it](mailto:piraino@idra.unipa.it)).

Flow over deformed bed of a meandering laboratory channel is experimentally investigated. The velocity components have been obtained using an Ultrasonic Doppler Profiler (DOP2000) that measures the instantaneous flow velocity profile along the probe direction. In this work, some results obtained in peculiar sections along the channel are reported. A refined mesh of the measurement points has been used for each considered cross-section. The analysis of the collected data essentially confirms that when the aspect ratio is small the secondary circulation assumes great importance and, in accordance with previous findings, a second counter-rotating secondary circulation cell appears near the free surface of the outer bank of the apex section. Such second circulation cell initiates at the bend entrance.

**Keywords:** Acoustic instrument, flow velocity field, secondary circulation, Reynolds stresses

## 1 INTRODUCTION

Accurate flow field measurements are necessary to analyze many stream processes, such as interaction flow-sediments, exchanges mechanism of sediments, nutrients and contaminants.

Because of the difficulty to obtain detailed flow velocity data by using traditional flow velocity meters, the analysis of turbulent structure of flow has been often limited. During the last decades, by developing laser and PIV sampling techniques, intensive experimental researches on the mechanism of turbulence production have been carried out [3-4]. But, very few experimental works have been conducted in order to analyze the secondary motion and the flow turbulence structure along a meandering bend.

In the present work detailed measures of flow velocity field in some sections of a large amplitude meandering channel have been carried out using an Acoustic Doppler Velocity Profiler (DOP 2000) by Signal Processing S.A. The instrument functioning is based on Doppler effect and consists of a probe that is simultaneously emitter and receiver of acoustic pulses; thus it allows to measure instantaneously the flow velocity profile along the probe direction. In order to analyze the interaction flow-sediment, from the instantaneous measured flow velocity vectors the turbulent fluctuation components as well as the turbulent stresses have been estimated.

The analysis has substantially confirmed the formation, in each apex section of the flume, of two circulation cells: the main circulation cell occurring in the central-region and a second counter-rotating circulation cell occurring near the free surface of the

outer bank. This second circulation cell strongly affects the turbulent activity and the distribution of the Reynolds stresses [1-2].

## 2 MEASUREMENT TECHNIQUE

The experimental installation has been constructed at the Dipartimento di Ingegneria Idraulica ed Applicazioni Ambientali, University of Palermo (Italy). The meandering channel follows the sine-generated curve with a deflection angle at the inflection section of 110°. The length of the meandering channel is of almost 27 m, i.e. equal to two meander wavelengths. The channel cross-section is rectangular with width  $B=0.50$  m; the banks are rigid and the bed is of quartz sand, with medium sediment diameter  $D_{50}=0.65$ mm and standard deviation  $\sigma_g=1.34$ . The initial longitudinal bed slope at the channel axis is of 0.371%. Other details of the experimental apparatus can be found in previous works [5-6].

The experiment has been conducted until the equilibrium bed topography was reached. The water discharge was  $Q=0.012$  m<sup>3</sup>/s and the average water depth at the channel centerline was  $h=5.5$  cm. At the end of the experiment the deformed bed was fixed by using cement dust. Then, the flow velocity measurements were carried out using the DOP 2000 in sections distant each other 50 cm or so. The acquisition frequency was of 4MHz and the pulse repetition frequency was variable in the range 5900-15600 Hz, depending on the local water depth and flow velocity. The distance between the center of adjacent sampling volumes was set equal of 0.75 mm; consequently, the number of emitted profiles

was included in the range  $500 \div 800$ . The acquisition time varied between 16.51 sec and 43.25 sec.

In order to obtain simultaneously the flow velocity components along the vertical ( $z$ ), the transverse ( $r$ ) and the longitudinal ( $s$ ) directions, three probes inclined of  $60^\circ$  with respect to the horizontal direction have been used.

Because each probe measures the instantaneous velocity vectors along its direction, the aforementioned velocity components have been determined through the vectorial composition of the measured vectors. For such purpose, a refined measurement mesh has been considered (see Figure 1). In the central area of the examined section (radial abscissa variable in the range 5 cm  $<r<$  45 cm) a measurement mesh with a step of 1.5 mm was used. As an example, Figure 2 shows the transverse and the vertical velocity components,  $V_r$  and  $V_z$ , obtained at the measurement point P of a cross-section.

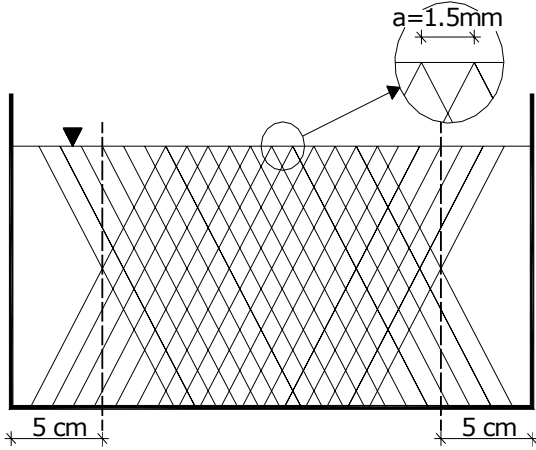


Figure 1: Measurement mesh

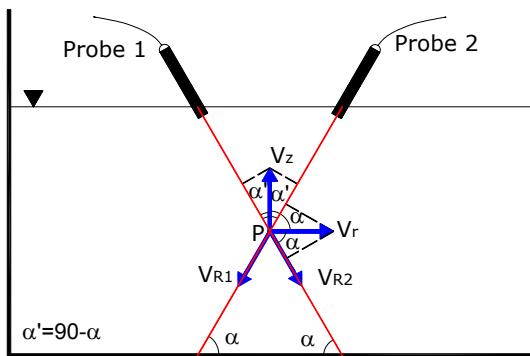


Figure 2: Measurement point P in the central zone of the cross-section.

$V_{R1}$  and  $V_{R2}$  are the velocity vectors measured at time  $t$  by probe 1 and probe 2, respectively. Thus, at point P,  $V_r$  and  $V_z$  have been obtained by solving the following system of equations:

$$V_{R1} = V_r \cdot \cos(\alpha) - V_z \cdot \sin(\alpha) \quad (1)$$

$$V_{R2} = -V_r \cdot \cos(\alpha) - V_z \cdot \sin(\alpha) \quad (2)$$

After simple passages it is:

$$V_r = \frac{V_{R1} - V_{R2}}{2 \cdot \cos(\alpha)} \quad (3)$$

$$V_z = -\frac{V_{R1} + V_{R2}}{2 \cdot \sin(\alpha)} \quad (4)$$

In the near-bank area, i.e. for a distance of 5 cm from each bank (see Figure 1), the probe nearest the bank was placed in vertical position as shown in Figure 3. In this case, the following system of equations has been solved:

$$V_{R1} = -V_z \quad (5)$$

$$V_{R2} = -V_r \cdot \cos(\alpha) - V_z \cdot \cos(\alpha) \quad (6)$$

The components  $V_r$  and  $V_z$  at point P has been obtained as:

$$V_r = -\frac{V_{R1} \cdot \sin(\alpha) - V_{R2}}{\cos(\alpha)} \quad (7)$$

$$V_z = -V_{R1} \quad (8)$$

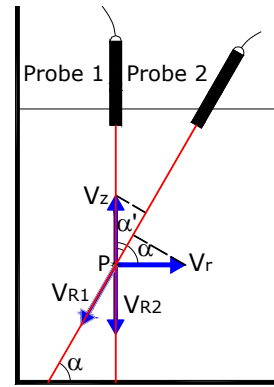


Figure 3: Measurement point in the near-bank area.

### 3 REYNOLDS STRESS DISTRIBUTION

In this paper the measurement sections reported in Figure 4 have been considered for the analysis.

For each measurement point, the Reynolds stresses  $\tau_{rZ} = -\rho \overline{v'_r v'_z}$ ,  $\tau_{rS} = -\rho \overline{v'_r v'_s}$ ,  $\tau_{zS} = -\rho \overline{v'_z v'_s}$ , (being  $v'_i$   $i=r, z, s$  the instantaneous fluctuation velocity component and the over-bar indicating the time-averaged values) have been estimated.

The contour lines of the estimated Reynolds stress components, normalized with respect to the mean shear stress  $\tau = -\rho u_*^2$  (being  $u_*$  the shear flow

velocity), are reported in Figures 5-7.

It can be observed from these figures that in both the apex sections (sections A and E) the cross-sectional Reynolds stress  $\tau_{rz}$  assumes different sign in the central region and in the outer bank region showing two peak values: one near the center of the cross-section and one near the free surface of the outer bank region. The component  $\tau_{zs}$ , that represents the shear stress acting on the vertical plane parallel to the banks, assumes a peak value near the free surface of the outer bank region. The component  $\tau_{rs}$ , that represents the shear stress acting on the horizontal plane, presents an alternance of sign inside the cross-section. It assumes the same sign (that is negative for section A and positive for section E) in the outer bank region and in the central region of the cross-section; such behaviour could be related to the evolution of turbulent structures in stream-wise direction. Furthermore, the maximum value of  $\tau_{rs}$  is found near the free surface of the outer region. Then, moving toward the outer bank it decreases in value assuming very low values very close to the outer bank.

As the curvature increases, i.e. passing from section A to section B, it can be observed that the distribution of each considered Reynolds stress component seems to be similar to that observed in the apex section A, but in section B the peak values of both the Reynolds components  $\tau_{rz}$  and  $\tau_{rs}$  occurring in the outer region seem to go away from the free surface and to decrease in magnitude.

In the inflection section (section C), where the channel curvature is maximum, all the three considered Reynolds stress components do not show evident peak values.

Passing from section C to section D, i.e. as the channel curvature decreases, it can be observed that for both the components  $\tau_{rz}$  and  $\tau_{rs}$  the contour-lines initiate to thicken in the outer bank region. Such behavior suggests that the outer bank circulation cell could initiate in this section.

#### 4 CONCLUSIONS

Acoustic Doppler Velocity Profiler has used to obtain detailed measures of flow velocity field in some sections of a large-amplitude meandering channel. From the measured flow velocity vectors, the Reynolds stresses  $\tau_{rz}$ ,  $\tau_{zs}$  and  $\tau_{rs}$  have been estimated. The analysis of the contour lines of these components has highlighted the formation of a counter-rotating outer-bank circulation cell near the free surface of each apex section. It seems that such circulation cell initiates at the bend entrance and decays approaching to the inflection section downstream.

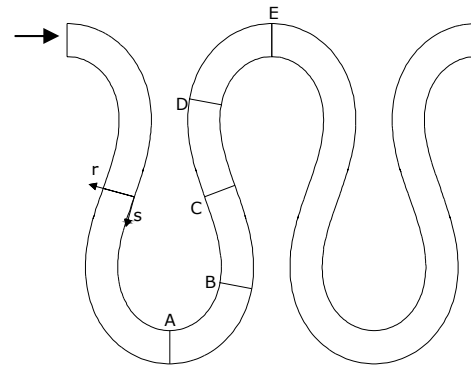


Figure 4: Measurement sections

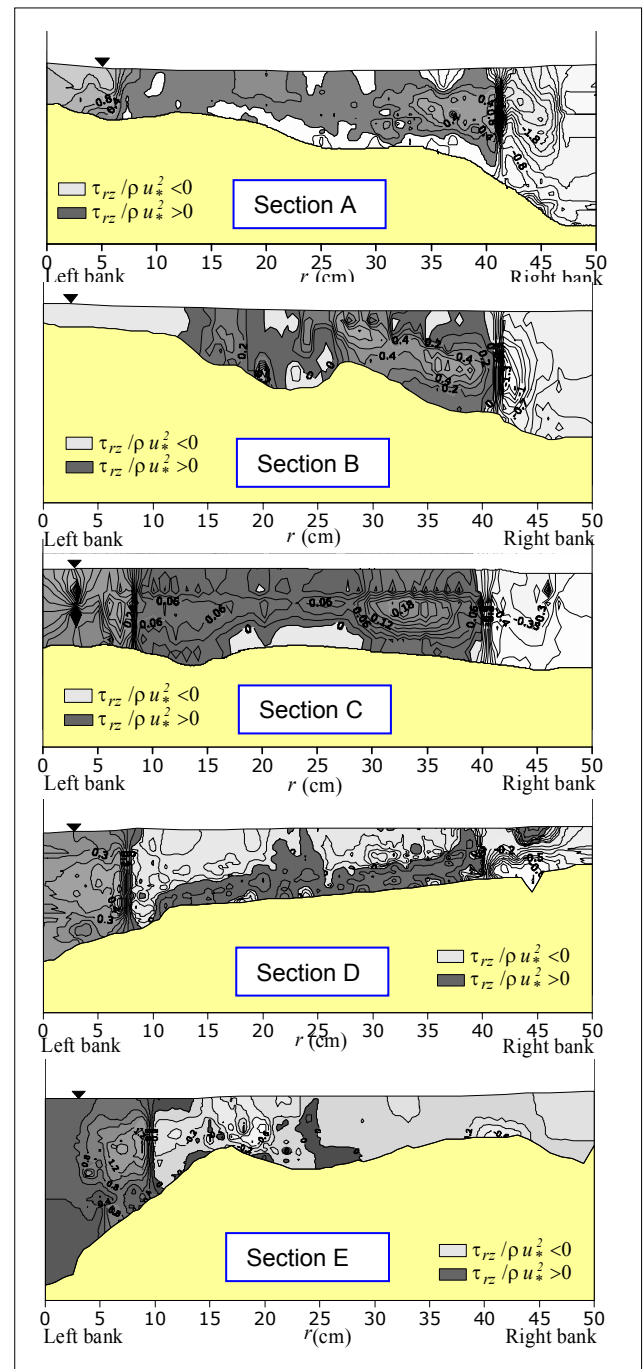


Figure 5: Normalized contour lines of  $\tau_{rz}/u_*^2$

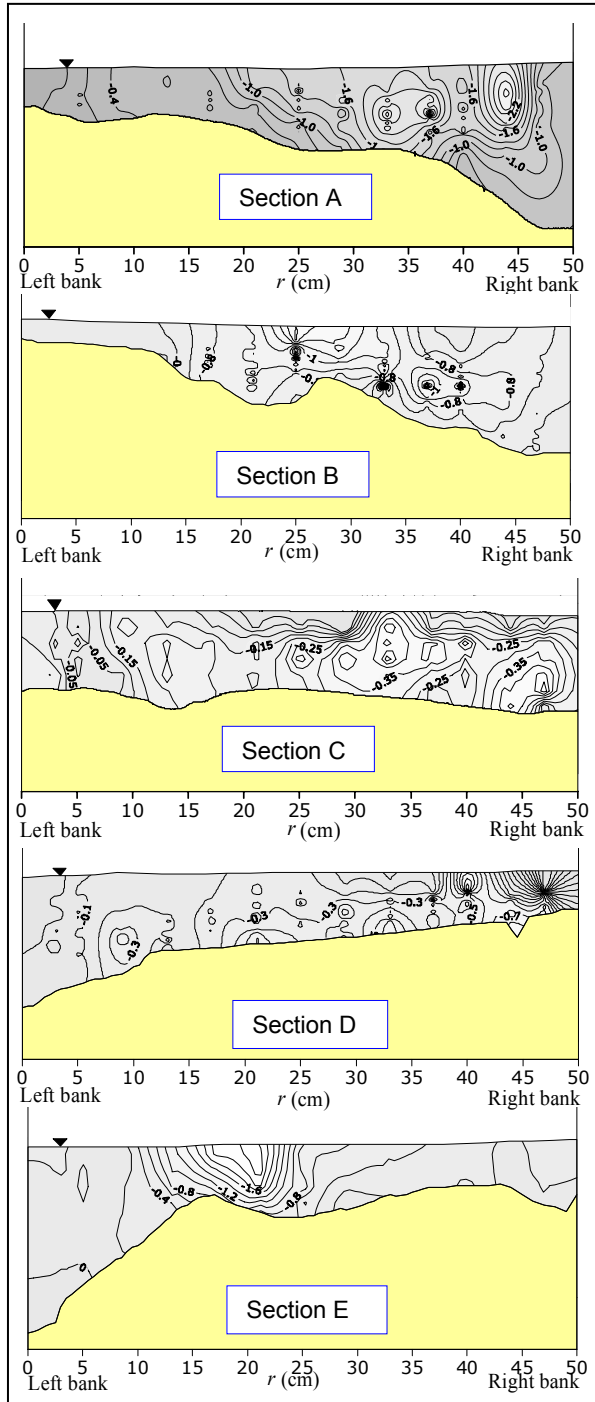


Figure 6: Normalized contour lines of  $\tau_{rs}/u_*^2$

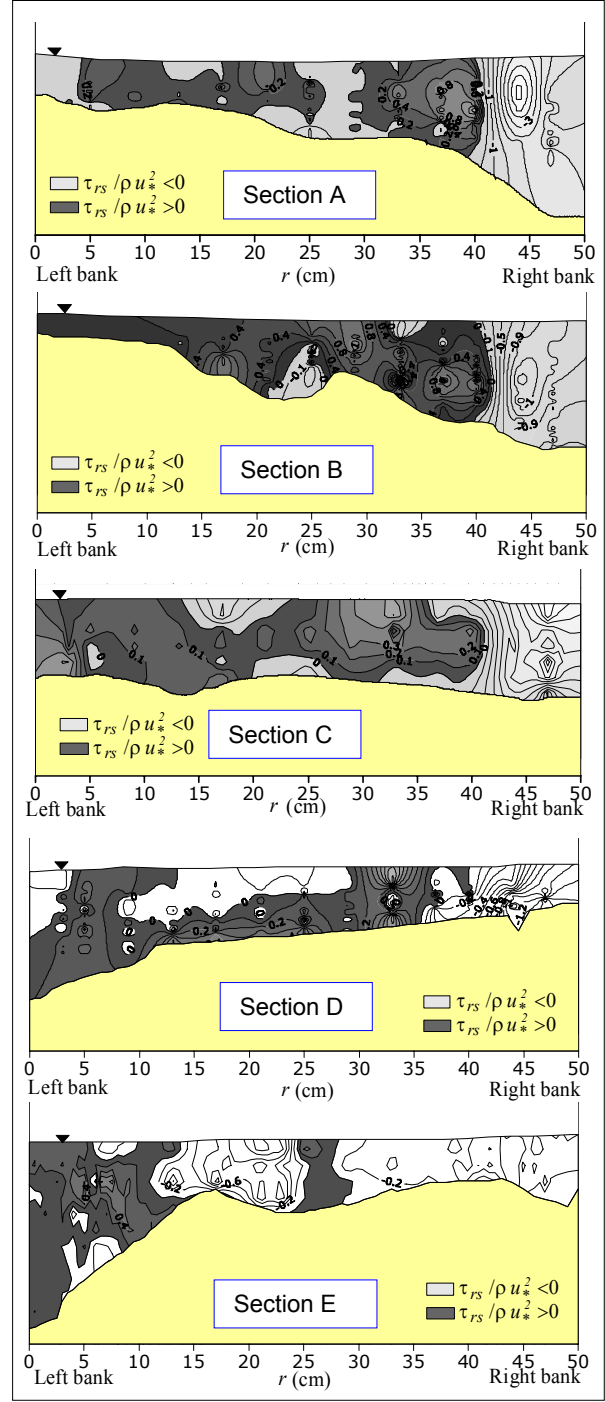


Figure 7: Normalized contour lines of  $\tau_{rs}/u_*^2$

**REFERENCES**

[1] Blanckaert K: Secondary currents measured in a sharp open-channel bends, International congress River Flow 2002, 4-6 September, Belgium (2002) 117-127.  
 [2] Booij R: Modelling of the secondary flow structure in river bends, International congress River Flow 2002, , 4-6 September Belgium (2002) 127-133.  
 [3] Cellino M, Lemmin U: Influence of coherent flow structures on the dynamics of suspended sediment transport in open-channel flow, Journal Hydraulic Engineering (2004) 1077-1088;

[4] Nino Y, Garcia M H: Experiments on particle-turbulence interactions in the near-wall region of an open channel flow: implications for sediment transport, Journal Fluid Mechanics. 326 (1996) 285-319.  
 [5] Termini D, Bonvissuto G, Piraino M: Analisi sperimentale delle caratteristiche cinematiche della corrente in un canale meandriforme di elevata ampiezza: primi risultati, XXIX Convegno di Idraulica e Costruzioni Idrauliche, Trento, 7-10 Settembre (2004) 555-562.  
 [6] Termini D, Piraino M: Secondary circulation motion in the apex section of a large amplitude meandering flume, 32nd congress of IAHR, Venice, 1-7 July (2007).